Nuclear Medicine & Biology, Vol. 26, pp. 149–157, 1999

ISSN 0969-8051/99/$–see front matter
PII S0969-8051(98)00069-9

Treatment of Lung Tumor Colonies with ^{90}Y Targeted to Blood Vessels: Comparison with the α-Particle Emitter ^{213}Bi

Stephen J. Kennel,[1] Michael Stabin,[2] Helio Yoriyaz,[3] Martin Brechbiel[4] and Saed Mirzadeh[1]

[1]LIFE SCIENCES DIVISION, OAK RIDGE NATIONAL LABORATORY, OAK RIDGE, TN 37831-6101, USA; [2]OAK RIDGE INSTITUTE OF SCIENCE AND EDUCATION, MEDICAL SCIENCES DIVISION, OAK RIDGE, TN 37831-0117, USA; [3]INSTITUTO DE PESQUISAS ENERGETICAS E NUCLEARES, IPEN-CN EN/SP, SAO PAULO, BRAZIL; AND [4]NATIONAL INSTITUTES OF HEALTH, NATIONAL CANCER INSTITUTE, DCS, BETHESDA, MD 20892, USA

ABSTRACT. An *in vivo* lung tumor model system for radioimmunotherapy of lung metastases was used to test the relative effectiveness of the vascular- targeted β-particle emitter ^{90}Y, and α-particle emitter, ^{213}Bi. Yttrium-90 was shown to be stably bound by CHXa″ DTPA-MAb 201B conjugates and delivered efficiently to lung tumor blood vessels. Dosimetry calculations indicated that the lung received 16.2 Gy/MBq from treatment with ^{90}Y MAb 201B, which was a sevenfold greater absorbed dose than any other organ examined. Therapy was optimal for ^{90}Y with 3 MBq injected. Bismuth-213 MAb 201B also delivered a similar absorbed dose (15Gy/MBq) to the lung. Yttrium-90 was found to be slightly more effective against larger tumors than ^{213}Bi, consistent with the larger range of 2 MeV β particles from ^{90}Y than the 8 MeV α particles from ^{213}Bi. Treatment of EMT-6 tumors growing in immunodeficient SCID mice with ^{90}Y or ^{213}Bi MAb 201 resulted in significant destruction of tumor colonies; however, ^{90}Y MAb 201B was toxic for the SCID mice, inflicting acute lung damage. In another tumor model, IC-12 rat tracheal carcinoma growing in SCID mouse lungs, ^{90}Y therapy was more effective than ^{213}Bi at destroying lung tumors. However, ^{90}Y MAb 201B toxicity for the lung limited any therapeutic effect. We conclude that, although vascular-targeted ^{90}Y MAb can be an effective therapeutic agent, particularly for larger tumors, in this model system, acute damage to the lung may limit its application. NUCL MED BIOL 26;1:149–157, 1999. **© 1998 Elsevier Science Inc.**

KEY WORDS. Lung, Tumor, β-Particle emitter, ^{90}Y, Yttrium-90

INTRODUCTION

For radioimmunotherapy (RIT) ^{90}Y has many advantages over other radioisotopes (7). It is readily available and can be stably attached to MAbs and other targeting proteins through bifunctional chelators (2, 16, 21, 23). It has a convenient half-life (64 h) and emits a 2 MeV β-particle, which generates a more uniform dose than α particles throughout the tumor (20).

Yttrium-90 has been used for successful preclinical studies in several tumor systems in which the radioisotope was targeted to tumor membranes (reviewed in 6). Recently, it has been shown that ^{90}Y-labeled monoclonal antibody (MAb) fragments are effective at curing small tumors with relatively few side effects (2).

The relative merits of α-particle emitters *vs.* β-particle emitters in various tumor settings has been discussed from a theoretical standpoint (32). In treatment of intraperitoneal tumors with radioisotope bound to microspheres, direct experimental comparisons show that the α-particle emitter ^{211}At was superior to ^{90}Y. Direct comparisons of MAb-targeted α- and β-particle emitters for RIT have not been reported, mostly because the short-lived α-particle emitters usually cannot be targeted to tumors quickly enough.

Recently, we developed a RIT model system wherein MAb to lung vascular endothelial cells is used to deliver radioisotopes to lungs bearing small tumor colonies (12, 15). The MAb accumulates to high concentrations within minutes of injection and thus promotes the use of radioisotopes with short half lives such as the α-particle emitter ^{213}Bi. In this system, the radioisotope is bound on the capillary endothelial surface and tumor cells grow perivascularly or in the deep lung. Bismuth-213 MAb has been shown to be effective in RIT of lung tumors if it is administered when tumors are small (10–12 cells in diameter), consisting of a few thousand cells each. Larger tumors showed growth retardation, but eventually progressed to lethal size. Theoretically, a high-energy β-particle emitter should be more effective in therapy of larger tumors, because the radiation can penetrate to distances of hundreds of cells from the origin of decay. Thus, ^{90}Y applied in RIT in the vascular targeting system should be capable of successful therapy of relatively large lung colonies.

To test this hypothesis, both radioisotopes were used in lung vascular-targeted RIT experiments for three different tumor types. The data show that ^{90}Y and ^{213}Bi were both effective in therapy of small tumors. Yttrium-90 was only marginally more efficient than ^{213}Bi in RIT of medium-sized tumors and like ^{213}Bi, was ineffective in killing larger tumors.

MATERIALS AND METHODS

The mammary carcinoma EMT-6 (9) was grown and injected into 4–6-week-old BALB/c female mice (Taconic Farms) as described previously (15). The rat tracheal carcinoma IC-12 (26) was grown and injected into 6–8-week-old ICR-SCID mice (15). Animals were housed in a specific pathogen-free facility at ORNL under

Address correspondence to: Dr. Stephen J. Kennel, Life Sciences Division, Oak Ridge National Laboratory, Bldg. 4500S, MS-6101, Oak Ridge, TN 37831-6101, USA; e-mail: sj9@ornl.gov.
Received 3 April 1998.
Accepted 30 May 1998.

protocol #0204 approved by the Institutional Animal Care and Use Committee.

MAb Labeling

MAb 201B reacting with murine thrombomodulin (13) and control MAb 14 with no known binding specificity were derivatized with freshly synthesized isomer a of cyclohexyl diethylenetriamine pentaacetic acid (CHXa″ DTPA) (4, 30) in solutions freed of metal by treatment with Chelex resin. The products were judged to have 4–6 chelator molecules/MAb (14). Bismuth-213 was eluted from an ^{225}Ac generator (3) with 200 μL 0.15 M HI, neutralized and reacted with CHXa″ DTPA-MAb for 6 min. Similarly, ^{90}Y (purchased from the radioisotope division of Pacific Northwest National Laboratory, Richmond, WA) was neutralized to pH 4.8 with 3 M NaOAc before addition to chelated MAb. Ethylene diamine tetraacetic acid (EDTA; 2 μL of 0.2 M) was added and the products diluted in MES buffer before analyses. The fraction of bound radioisotope was judged by centrifugation of the reaction product in Microcon 30 filter units (Millipore Labs). The retained fraction (bound to MAb) ranged from 83 to 88% for ^{213}Bi and 93 to 94% for ^{90}Y.

Cells and Animal Studies

Cells were used after one *in vitro* growth cycle following recovery from frozen storage. Cells were harvested by treatment with trypsin-EDTA, diluted into growth media containing 10% fetal bovine serum, counted in a hemocytometer, collected by centrifugation, suspended in phosphate-buffered saline (PBS) at the appropriate concentration, and injected (200 μL intravenously) within 30 min of harvest.

At stated times after cell injection, animals were treated by IV injection of radiolabeled MAb. For therapy experiments, treated animals were observed daily and sacrificed for histologic examination when moribund. Animals were considered moribund if they were lethargic and demonstrated labored breathing. In addition, animals losing greater than 20% of their body weight or with external tumors greater than 1 cm in diameter were sacrificed. Lung colonies were quantitated in stained, 5-μm lung sections as described previously (12). Yttrium-90 MAb distribution was monitored as described previously (12). Briefly, animals were sacrificed and target organs were removed, weighed, and analyzed for ^{90}Y by counting brehmstrahlung radiation in a NaI gamma detector.

Mouse Model for Radiation Dose Estimates

A model of a 30-g mouse was developed using approximate geometrical shapes to represent the whole body and various organs (31). The body was modeled as an ellipsoid with axes of length 1.5, 1.5, and 3.1 cm:

$$\left(\frac{x}{1.5}\right)^2 + \left(\frac{y}{1.5}\right)^2 + \left(\frac{z}{3.1}\right)^2 \le 1$$

Within the mouse model, the following organs were also described:

Liver: modeled as an ellipsoid with axes of length 0.582, 1.118, and 0.582 cm:

$$\left(\frac{x}{0.582}\right)^2 + \left(\frac{y}{1.118}\right)^2 + \left(\frac{z - 0.400}{0.582}\right)^2 \le 1$$

TABLE 1. Mass and Volume of the Organs and Total Body of a 30-g Mouse

Organ	Volume (cm^3)	Mass (g)
Lung	0.47	0.139 (0.130)[a]
Liver	1.284	1.335 (1.84)
Kidneys	0.276	0.287 (0.40)
Intestines	3.824	3.977 (4.24)
Heart	0.148	0.154 (0.14)
Stomach	0.183	0.190 (0.16)
Remainder	23.022	23.943
Total	29.207	30.026

[a] The values in parentheses are literature values (18, 25).

and cut by planes: $z = 0.8$ cm; $0.866x + 0.5z = -0.16$; and $z = -0.05$ cm.

Lungs: modeled as ellipsoids with axes of length 0.40, 0.40, and 0.80 cm:

$$\left(\frac{x}{0.400}\right)^2 + \left(\frac{y \pm 0.300}{0.400}\right)^2 + \left(\frac{z - 1.000}{0.800}\right)^2 \le 1$$

and cut by planes: $z = 0.8$ cm; $y = 0.0$ cm; and $x = 0.1$ cm.

Intestines: modeled as cylinder with diameter of 1.78 cm and length of 1.64 cm:

$$\left(\frac{x}{0.890}\right)^2 + \left(\frac{z + 1.10}{0.890}\right)^2 \le 1$$

and cut by the plane $z = -0.35$ cm.

Kidneys: modeled as ellipsoids with axes of length 0.33, 0.33, and 0.375 cm:

$$\left(\frac{x + 0.460}{0.330}\right)^2 + \left(\frac{y \pm 0.420}{0.330}\right)^2 + \left(\frac{z}{0.375}\right)^2 \le 1$$

and cut by planes: $0.866x + 0.5z = -0.16$ and $0.5x - 0.866z = -0.03$.

Heart: modeled as an ellipsoid with axes of length 0.25, 0.60, and 0.55 cm:

$$\left(\frac{x - 0.100}{0.250}\right)^2 + \left(\frac{y - 0.100}{0.600}\right)^2 + \left(\frac{z - 1.100}{0.550}\right)^2 \le 1$$

cut by planes: $x = 0.1$ cm and $z = 0.8$ cm.

Stomach: modeled as an ellipsoid with axes of length 0.40, 0.60, and 0.36 cm:

$$\left(\frac{x + 0.030}{0.400}\right)^2 + \left(\frac{y - 0.100}{0.600}\right)^2 + \left(\frac{z + 0110}{0.360}\right)^2 \le 1$$

cut by planes: $0.5x - 0.866z = -0.03$ $z = -0.05$ cm and $z = -0.35$ cm. The masses and volumes of the structures in this model are based on the data from the literature (18, 25), and are shown in Table 1.

The MCNP-4A code (5) was run to simulate the transport of both the electrons and photons. Enough histories were run to obtain good statistics on the reported results; typically about 500,000 particle histories were accumulated. Absorbed fractions and S-

TABLE 2. Tissue Distribution and Dosimetry of ^{90}Y MAb

	Time					Dose[b] (Gy/MBq)		
	1 hr	4 hr	12 hr	24 hr	72 hr	Self	Cross	Total
%ID/g of specific MAb 201B[a]								
Blood	1.05 ± 0.07	1.2 ± 0.05	1.3 ± 0.02	0.9 ± 0.02	1.3 ± 0.08	NC[d]	NC	NC
Muscle	0.50 ± 0.06	0.57 ± 0.02	0.46 ± 0.01	0.41 ± 0.01	0.33 ± 0.02	NC	NC	NC
Liver	2.1 ± 0.1	2.7 ± 0.2	3.2 ± 1.0	2.7 ± 0.1	4.4 ± 1.0	1.50	0.99	2.49
Spleen	2.4 ± 0.9	3.2 ± 0.6	4.2 ± 0.4	5.0 ± 0.9	6.5 ± 0.4	1.25	NC	1.25
Kidney	5.1 ± 1.0	5.1 ± 0.2	4.2 ± 0.07	3.8 ± 0.6	2.5 ± 0.7	0.79	0.17	0.96
Lung	322 ± 3	316 ± 21	286 ± 40	243 ± 6	155 ± 30	15.9	0.26	16.2
%ID/g of control MAb 14[c]								
Blood	39.8 ± 4.5			28.9 ± 2.7	24.5 ± 8	NC	NC	NC
Muscle	1.8 ± 1.0			1.5 ± 0.1	1.8 ± 0.2	NC	NC	NC
Liver	11.8 ± 0.4			9.3 ± 1.7	9.0 ± 3.5	3.81	0.11	3.92
Spleen	9.0 ± 2.7			7.2 ± 1.2	10.4 ± 0.4	2.06	NC	2.06
Kidney	9.1 ± 4.5			6.5 ± 0.2	6.8 ± 0.6	1.84	0.42	2.26
Lung	11.6 ± 1.2			7.5 ± 0.2	8.7 ± 0.6	0.68	0.65	1.33

[a] 8-week-old normal BALB/c mice were injected with 1.0 μg of MAb 201B with CHXa″ chelated ^{90}Y (0.43 MBq/μg) at 93% radioistope bound (4/1/97). Two animals were sacrificed at each time point. Average organ weights were: lung = 0.123 ± 0.014 g; spleen = 0.113 ± 0.01 g; kidneys (2) = 0.310 ± 0.07, g.
[b] Calculated from MIRDOSE adjusted for the mouse model defined in this paper.
[c] As above except MAb14 (1.0 μg at 0.37 MBq/μg) at 94% radioisotope bound.
[d] Not calculated.

values (17) were generated for sources in all major organs and the "remainder of the body." Bismuth-213 decay to ^{213}Po, ^{209}Tl, and ^{209}Pb produces α particle, β particle, and γ ray radiation, whereas ^{90}Y produces only β particles. Retention data for the compounds in the mouse organs were fitted to one or two component exponential functions using the SAAM II software (8). Areas under the time–activity curves were combined with the specially calculated dose conversion factors (S values) calculated using the MCNP

TABLE 3. Activity Response for Treatment of EMT-6 Tumors in BALB/c Mice with ^{90}Y or ^{213}Bi MAb Time to Sacrifice (days + SD)

		Radioactivity injected (MBq)						
Treatment	Group	0	0.37	0.93	1.85	3.7	7.4	11.1
Experiment 1[a]								
^{90}Y MAb 201B	1	17.3 ± 8 (4/4)	16.6 ± 2.5 (5/5)	21 ± 6 (4/4)	35 ± 11[b] (4/5)	51 ± 12[b] (0/6)	48 ± 7 (0/5)	24 ± 6 (0/5)
^{90}Y MAb14	2	ND	17 ± 9 (4/4)	15 ± 3 (5/5)	ND	17 ± 3 (5/5)	ND	19 ± 1 (4/5)
^{90}Y EDTA	3	ND	ND	ND	ND	16 ± 2 (5/5)	ND	13 ± 2 (5/5)
^{90}Y MAb 201B (no tumors)	4	ND	ND	ND	>200[c]	ND	ND	20 ± 1

		Radioactivity injected (MBq)			
		0.37	0.93	2.78	3.7
Experiment 2[d]					
^{90}Y MAb 201B	5	14.8 ± 1.6	15.6 ± 1.8	111 ± 46[e]	51.4 ± 2.3
^{213}Bi MAb 201B	6	14.4 ± 1.9	21 ± 7	25 ± 1.9	42 ± 17
^{90}Y MAb 14	7	12.6 ± 0.5	13 ± 1	ND	16.2 ± 3.3
^{213}Bi MAb 14	8	12.8 ± 1.1	14 ± 1.7	ND	16.6 ± 2.5

[a] Animals injected with 2×10^4 (p10) EMT-6 cells (3/29/97). Treated on day 5 with ^{90}Y MAb (0.43 MBq/μg MAb). Data are presented as time to sacrifice of animals in days ± SD. Animals surviving >200 days were not included in the averages. Numbers in parentheses indicate animals with lung tumors/number tested.
[b] One long-term survivor (>200 days).
[c] All animals (5/5) surviving >200 days.
[d] Animals injected IV with 2×10^4 p10 EMT-6 cells (7/10/97). Treatment on day 5 after cell injection with CHXa″-MAb 201B or MAb14 chelated with ^{213}Bi at 0.58 MBq/μg MAb 201 or MAb14 (87% radioisotope bound) or with ^{90}Y at 0.60 MBq/μg MAb (93% radioisotope bound).
[e] Two animals surviving at 150d.
Time to sacrifice for control groups not shown in the table were: animals not treated, treated with 3.7 MBq ^{90}Y EDTA or ^{213}Bi EDTA were 12.3 ± 1.0, 12.8 ± 0.8, 13.2 ± 1.1 d, respectively.

TABLE 4. Treatment of EMT-6 Tumors of Different Sizes with ^{90}Y or ^{213}Bi MAb

Day[b]	Treatment	Tumor incidence (# positive/ # tested)	Time to sacrifice of LT positive mice (d ± SD)
Experiment 1[a]			
5	^{90}Y MAb 201B	2/4	35 ± 4
6	^{90}Y MAb 201B	0/5	—
6	^{90}Y MAb 14	5/5	16 ± 2
6	^{90}Y EDTA	5/5	13 ± 1
7	^{90}Y MAb 201B	0/5	—
8	^{90}Y MAb 201B	5/5	18 ± 7
Experiment 2[c]			
5	^{90}Y MAb 201B	0/10	—
5	^{213}Bi MAb 201B	3/10	28.1 ± 12
6	^{90}Y MAb 201B	0/10	—
6	^{213}Bi MAb 201B	5/10	20.4 ± 0.5
6	^{90}Y MAb 14	5/5	13.6 ± 0.5
6	^{213}Bi MAb 14	5/5	13.2 ± 1.1
6	^{90}Y EDTA	5/5	12.8 ± 0.8
6	^{213}Bi EDTA	5/5	12.6 ± 1.3
7	^{90}Y MAb 201B	1/5	27
7	^{213}Bi MAb 201B	5/5	17.4 ± 2.3
8	^{90}Y MAb 201B	5/5	18.5 ± 3.8
8	^{213}Bi MAb 201B	5/5	14.4 ± 1.5

[a] Female BALB/c mice age 7–10 weeks, bred in the Oak Ridge facility were injected with 2×10^4 (p10) EMT-6 cells IV (3/29/97). Mice were treated with CHXa″ DTPA MAb chelated with 3.8–4.4 MBq ^{90}Y at 0.26 MBq/μg MAb at the day indicated.
[b] For tumor sizes at the time of treatment, see Fig. 1.
[c] Female BALB/c mice age 4–5 wks (Taconic Farms) were injected with 2×10^4 (p10) EMT-6 cells IV (7/10/97). Mice were treated with CHXa″ DTPA MAb chelated with either 2.6 MBb ^{90}Y at 0.4 MBq/μg MAb or with 2.8 MBq ^{213}Bi at 0.46 MBq/μg MAb.

software (5). Total absorbed doses were calculated for all important target organs, considering all sources of radiation dose. The fractional contribution from cross-irradiation of different organs by electrons was calculated. Spleen was not explicitly defined in the mouse model. Self-doses for spleen from alpha and beta were calculated, assuming a spherical geometry and a spleen mass observed in measurements from the animals employed in the distribution studies. Absorbed fractions for alpha particles were assigned to be unity; for betas, the absorbed fractions of Siegel and Stabin (24) were used. The mass of the spleen was 0.113 g. Most of the absorbed dose from ^{213}Bi is from α particles. The absorbed dose of β particles from ^{213}Bi decay to ^{213}Po was less than 5% of the α contribution (12). The dose from ^{209}Pb decay is somewhat less than this amount, because Pb is released from CHXa° DTPA into the circulation and at least partially excreated (unpublished data).

RESULTS

Radioisotope Distribution and Dosimetry

Previous work has documented that MAb 201B-CHXb-DTPA was efficient in delivery of ^{213}Bi to lungs of BALB/c or SCID mice bearing experimental lung tumors (12). Others have shown that the isomer CHXa″ DTPA is a better chelating agent for ^{90}Y (30). Yttrium-90 chelated to CHXa″ DTPA-MAb 201B was shown to accumulate rapidly in lung, whereas ^{90}Y chelated to control MAb 14 remained largely in the circulation with small levels of accumulation in liver, kidney, spleen, and lung (Table 2). The ^{90}Y bound to the lung was retained there ($t_{½}$ = ~65 h). These data indicate that, like ^{213}Bi, the ^{90}Y-CHX-DTPA complex is very stable in physiologic conditions.

The distribution data were used to calculate absorbed doses of ^{90}Y to various tissues in the mouse. In this targeting system, the dose of ^{90}Y β particles to the lung (16.2 Gy/MBq) was more than seven times greater than the absorbed dose to any other organ. The 'cross doses' from the lung to other organs were small with the exception of the liver (Table 2). The present mouse model has considered the overlapping area, F_{kh}, between the organs, as also studied by Hui *et al.* (10). The ratios of overlapping surface area of target and source organs to the surface area of the source organ were calculated. The shapes were modified in an attempt to be similar to the values of F_{kh} reported by Hui *et al.* (10). Yttrium-90 bound to the control MAb 14 resulted in moderate doses (4 Gy/MBq) to liver with lesser doses to kidney, spleen, and lung.

Dose–Response

To determine if ^{90}Y MAb 201B was effective in the system of vascular targeted RIT, BALB/c mice bearing small lung colonies of EMT-6 tumor cells were treated with different amounts of radiolabelled MAb (Table 3, Experiment 1). Mice in groups treated with control ^{90}Y MAb 14 (Group 2) or ^{90}Y chelated with EDTA and mixed with MAb 201B (Group 3) died in less than 20 days. All had massive lung tumor burden (data not shown). In contrast, treatment with ^{90}Y MAb 201B (Group 1) at all doses greater than about 1 MBq (~15 Gy to the lung) resulted in extended life span and destruction of the majority of lung tumors. Animals treated with 3.7 MBq of ^{90}Y MAb 201B (Group 1) had significant damage to normal lung, which was ultimately the cause for their sacrifice. Animals not bearing tumors, but injected with 11.1 MBq of ^{90}Y MAb 201B (Group 4), also had lung damage and had similar life spans as those in the tumor-bearing group (Group 1) that were cured of lung tumors.

A second experiment was done to confirm these results and to compare ^{213}Bi and ^{90}Y directly (Table 3, Experiment 2). In this experiment, EMT-6 tumors were slightly more aggressive (test animals were younger at injection) and control animals all died with life spans of 12–16 days. All animals treated with 3.7 MBq of ^{90}Y MAb 201B were cured of lung tumors but died of complications due to lung damage. Tumor cures with ^{213}Bi MAb 201B in this experiment were not as complete as in previous experiments (12); however, the data showed a statistically significant dose–response effect. As with ^{90}Y, animals treated with 3.7 MBq of ^{213}Bi were all cured of lung tumors but died of radiation-induced lung damage. The total absorbed dose to the lung for ^{90}Y and ^{213}Bi was similar (~15 Gy/MBq); however, the dose rate for ^{213}Bi was about 80-fold higher. Dose calculations did not include microdosimetry for ^{213}Bi α-particle emissions.

Tumor Size at Treatment

Because the β particle from ^{90}Y penetrates much further than the α particle from ^{213}Bi, ^{90}Y should be more effective at therapy of larger tumors. In two experiments, tumors were allowed to grow to larger sizes before treatment with ^{90}Y or ^{213}Bi MAb. Data in Table 4, Experiment 1, indicate that ^{90}Y MAb 201B was effective at curing lung tumors up to 7 days postinjection of cells. These results are similar to those obtained with ^{213}Bi MAb 201B in previously published work (15). Figure 1 (right side panels) presents photomicrographs of lung histologic sections indicating the size of the

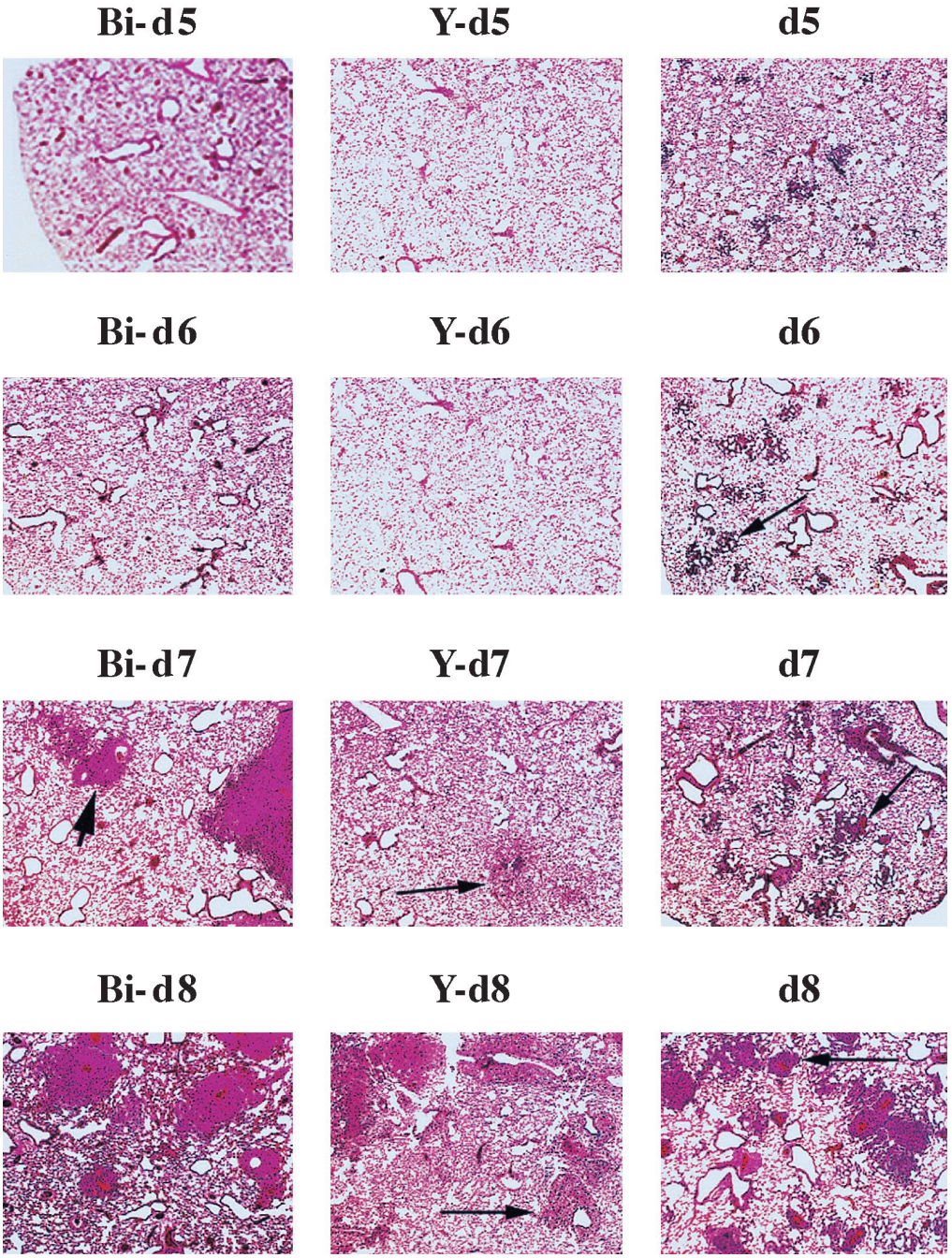

FIG. 1. Histologic analyses of EMT-6 lung colonies of different sizes treated with 2.8 MBq ^{90}Y or ^{213}Bi MAb 201B (Table 4, Experiment 2). Panels on the right show the size of the tumors at time of treatment. Female BALB/c mice were injected intravenously (IV) with 2 × 10^4 EMT-6 cells and treated with ^{90}Y MAb 201B (center panels) or ^{213}Bi MAb 201B (left panels) (see legend Table 4 for details). Animals treated with MAb were sacrificed when moribund. Histology sections from animals treated at day 5 (d5) with ^{90}Y or ^{213}Bi (sacrificed on d73 and d54, respectively); treated at d6 (sacrificed on d77 and d60); treated at d7 (sacrificed on d46 and d21); treated at d8 (sacrificed on d24 and d18). Magnification approximately 30×. Representative tumor colonies are indicated by short arrows. Longer arrows in Y-d7 and Y-d8 indicate tumor colonies with dying cells.

tumors at the times of treatment. It was estimated that each animal developed about 100 original lung colonies, which contained averages of 250 cells on day 5, 500 cells on day 6, 2,000 cells on day 7, and 5,000 cells on day 8. These data are consistent with previous measurements in the EMT-6 lung colony system (15).

In Experiment 2, Table 4, in which alternate groups of animals were treated with ^{90}Y or ^{213}Bi MAbs, ^{90}Y was more effective. In this experiment, mice were only 4–5 weeks old at injection and control animals died of lung tumors earlier than in previously published works, in which animals were 6–8 weeks old at initiation of treatment. Fewer animals were totally cured of lung tumors. Even though no animals were cured of lung tumors with ^{213}Bi MAb 201B

TABLE 5. Treatment of EMT-6 Tumors in SCID Mice with ^{90}Y MAb[a]

MAb	Radioactivity injected (MBq)	*n*	Tumor/lung section	Time to sacrifice (d ± SD)
MAb 201B	3.7	5	34 ± 17	16 ± 1.2
MAb 14	3.7	5	77 ± 42	15 ± 2
EDTA	3.7	5	170 ± 43	14.2 ± 0.4
MAb 201B	0.93	3	149 ± 45	14.3 ± 0.6
MAb 14	0.93	3	157 ± 20	13.6 ± 0.6

[a] Female ICR-SCID mice (Taconic Farms) were injected IV with 2×10^4 EMT-6 (p11) and treated on day 5 with CHXa″-MAb with ^{90}Y (93% radioisotope bound) at 0.26 MBq/μg MAb (3/29/97).

TABLE 6. Treatment of IC-12 Tumors in SCID Mice with ^{90}Y or ^{213}BiMAb

Group	Treatment	Radioactivity injected (MBq)	*n*	Time to sacrifice (d ± SD)
Experiment 1[a]				
1	^{90}Y MAb 201B	4.5	5	26 ± 7
2	^{90}Y MAb 14	4.2	4	18 ± 3
3	^{90}Y EDTA	4.2	5	21 ± 2
Experiment 2[b]				
4	^{90}Y MAb 201B	2.8	5	21.1 ± 1.3
5	^{213}Bi MAb 201B	2.8	5	3.2 ± 3.4
6	^{90}Y MAb 14	2.8	5	19.6 ± 1.1
7	^{213}Bi MAb 14	2.8	5	23.8 ± 3.4
8	MAb 201B	—	5	24 ± 2

[a] Male ICR-SCID mice injected IV with 10^6 IC-12 cells (p33) (3/29/97) and treated on day 5 with CHXa″ MAb 201B or 14 with ^{90}Y (94% radioisotope bound) at 0.26 MBq/μg MAb. Statistical significance: grp 1 *vs* grp 2 (p = 0.025) grp 1 *vs*. grp 3 (p = 0.05).
[b] Female ICR-SCID mice injected IV with 10^6 IC-12 cells (p35) (7/9/97) and treated on day 6 with CHXa″ MAb 201B or 14 chelated with ^{90}Y (93% radioisotope bound) at 0.43 MBq/μg MAb or ^{213}Bi (83% radioisotope bound) at 0.38 MBq/μg MAb. Significance of ^{90}Y effect, grp 4 *vs*. grp 6 or 8, NS. Significance of ^{213}Bi effect, grp 5 *vs*. grps 7 or 8, $p < 0.001$. ^{90}Y grp 4 *vs*. ^{213}Bi grp 5, $p < 0.001$.

treatment at day 7, tumor growth was somewhat retarded as indicated by the slight increase in life span (17 *vs*. 13 days). At estimated tumor growth rates, this correlates with about 90% tumor cell killing. To evaluate the cellular response of radioimmunotherapy of the two radioisotopes in the lung, lungs were taken for histology at the times of sacrifice (when animals were moribund). Data shown are for animals described in Table 4, Experiment 2. Stained sections of lung, representative of the whole treatment group, are shown in Figure 1, ^{213}Bi MAb 201B treated (left panels) or ^{90}Y MAb 201B treated (center panels). All of the animals treated with ^{90}Y and most of the animals treated with ^{213}Bi at days 5 or 6 had no evidence of residual lung tumors at the time of sacrifice. The largest differences in radioisotope effect was noted in animals treated at day 7 (d7) when tumors were about 2,000 cells in size. Most of the animals treated with ^{90}Y were cured of lung colonies (panel Y-d7) whereas all of the animals treated with ^{213}Bi in this parallel experiment had viable lung tumor colonies at the time of sacrifice (Fig. 1, panel Bi-d7). Animals cured of lung colonies with ^{90}Y MAb 201B injected at d7 all died with lung damage (37 ± 8 days). All animals treated at day 8 (d8) with either radioisotope died early (14–18 days) with large lung tumor burden (panel Bi-d8), although some of the tumor colonies in the ^{90}Y-treated animals appeared necrotic (panel Y-d8).

Treatment of Tumors in SCID Mice

Previous work has shown that SCID mice bearing EMT-6 lung colonies had extended life spans and 10-fold fewer lung tumors when treated with ^{213}Bi MAb 201B. The efficacy of ^{90}Y MAb 201B was tested in the same system. Data in Table 5 show that ^{90}Y MAb 201B was capable of reducing the lung tumor burden about three- to fivefold relative to controls when administered at 3.7 MBq/animal. Lower doses were not as effective, as the reduction of tumor burden did not result in extended life span of the animals. These data and other work (see Table 6) have shown that ^{90}Y MAb 201B is very toxic for SCID mice. Doses that are tolerated in BALB/c mice for up to 3 months are lethal in SCID mice in about 25 days (data not shown). These animals experienced acute lung damage due to the treatment; however, the cause of death of these animals was not firmly established, even after histologic examination.

Treatment of IC-12 rat tracheal carcinomas growing in lungs of SCID mice were also complicated by the toxicity of ^{90}Y MAb 201B (Table 6, Experiment 1). SCID mice bearing IC-12 tumors showed evidence of tumor destruction (Fig. 2, panels B and F) when treated with 4.5 MBq of ^{90}Y MAb 201B, but these animals had only slightly increased life spans (26 ± 7 days *vs*. 18 ± 3 days; p = 0.05) (Table 6, Experiment 1) or life spans which were not significantly different when treated with 2.8 MBq of ^{90}Y MBq MAb 201 (21.1 ± 1.3 days *vs*. 19.6 ± 1.1 days; $p > 0.2$. (Table 6, Experiment 2). In comparison, treatment with ^{213}Bi MAb 201B significantly reduced tumor burden (Fig. 2, panels A and E) and increased life span of the animals over those treated with ^{213}Bi MAb14 (controls) and over ^{90}Y MAb 201B-treated animals ($p < 0.001$). The enhanced life span of these animals is consistent with other published results with ^{213}Bi MAb 201B treatment of IC-12 tumors in SCID mice (15).

To determine the status of the lungs of treated ICR-SCID mice at the time of their sacrifice, stained histologic sections were prepared (Fig. 2). Sections from all animals receiving control MAb with either ^{90}Y (panels B and F) or ^{213}Bi (panels D and H) died with massive lung tumor burden. Treatment of ICR-SCID mice with ^{213}Bi MAb 201B (panels C and G) resulted in reduced tumor burden, but all animals ultimately died of lung tumors. Mice treated with ^{90}Y MAb 201B (panels A and E) had few if any residual lung tumors at the time of sacrifice, but they died very early with acute lung damage.

DISCUSSION

The purpose of this work was to compare the efficiency in vascular targeted RIT of high energy α- and β-particle emitters in an animal model. Yttrium-90 exclusively emits a 2-MeV β particle ($E\beta^{AV}$ = 0.935) that can penetrate an average of 0.7 cm in tissue, depositing 0.2 KeV/μm. Bismuth-213 decay results mainly in emission of an α particle (8.4 MeV) that can penetrate 70–100 μm in tissue, depositing about 100 KeV/μm. For the purpose of this discussion, other emissions α, β, and γ from the ^{213}Bi decay chain can be neglected as they comprise less than 5% of the total dose. Several studies have been done to estimate the number of hits to cell nuclei and the energy deposited per nuclear transversal (22). Humm *et al.* (11) calculated that, for radioisotope bound to a single cell, the α-particle emitter ^{211}At would be 1,000 times more toxic than the β-particle emitter ^{90}Y. Experimental work on cells in culture (data

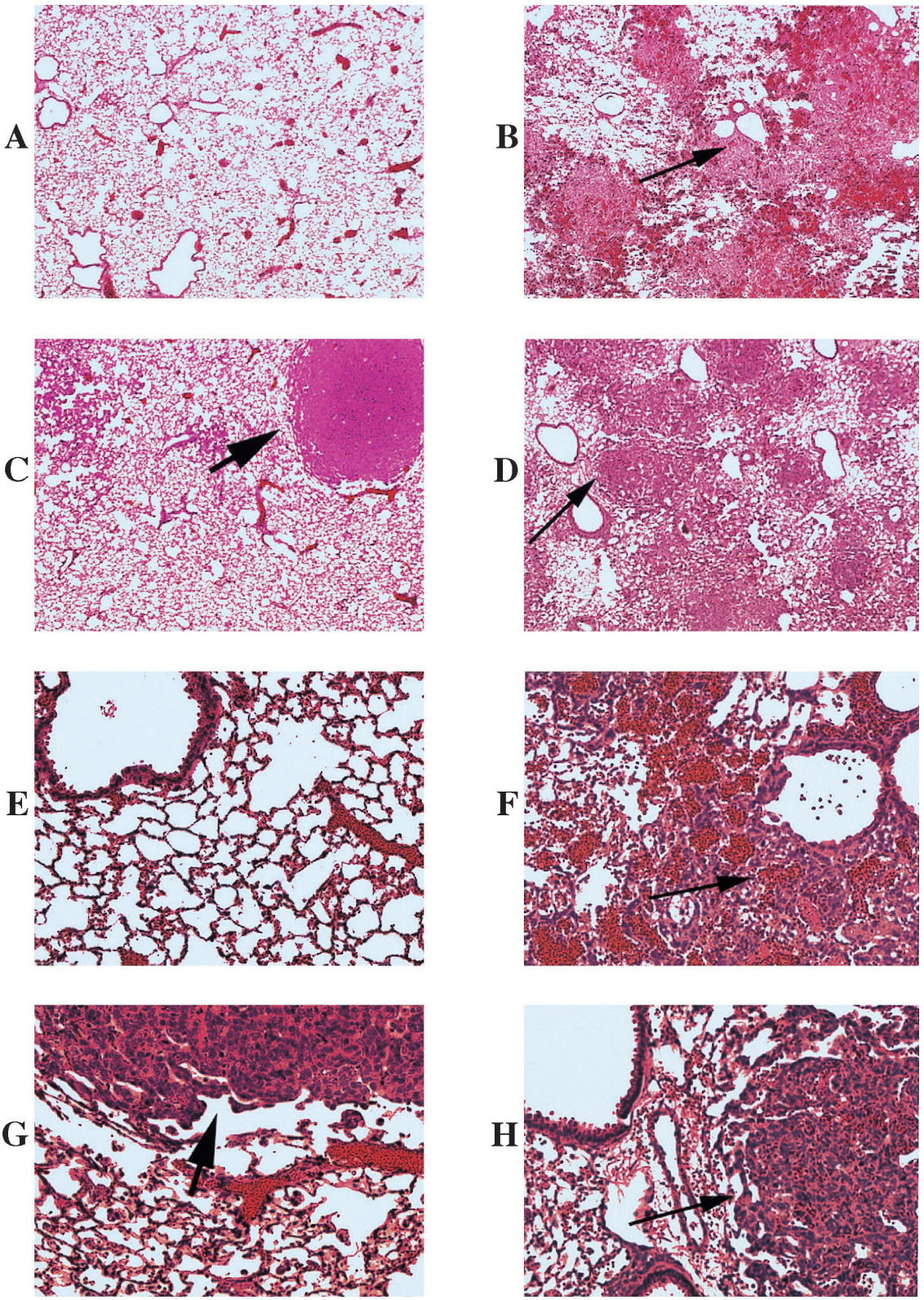

FIG. 2. Comparison of histologic lung sections from SCID-ICR mice bearing IC-12 colonies treated with 2.8 MBq ^{90}Y or ^{213}Bi MAb (Table 6, Experiment 2). All animals treated on day 6 (d6) after cell injection with ^{90}Y MAb 201B, d21 (panels A and E); ^{90}Y MAb 14, d19 (panels B and F); ^{213}Bi MAb 201B, d26 (panels C and G); or ^{213}Bi MAb 14, d21 (panels D and H). Panels A–D, magnification approximately 30×; Panels E–H, magnification approximately 150×. Tumor colonies are indicated by short arrows. Longer arrows indicate tumors in control treated animals.

not shown) confirms the advantage of α particles over β particles at short range.

Data on dose–response (Table 3) and previous work (12) indicate that injected activities of 1–2 MBq of either ^{213}Bi or ^{90}Y targeted to the mouse lung vessels were about equally effective in therapy of small tumor nodules (day 5, 200–400 cells). Absorbed dose calculations indicate that the dose to the lung is similar per MBq of either radioisotope injected (Table 2; 12). This is because ^{90}Y has a larger number of accumulated disintegrations per Bq than ^{213}Bi due to its longer $t_{1/2}$ but has a lower linear energy transfer and thus lower absorbed energy per path length than for ^{213}Bi. These two characteristics counteract one another in the absorbed dose calculations. The absorbed doses required for cure of these small tumors are about 30 Gy. Local doses of α particles may be much higher and the dose rate from ^{213}Bi is about 80-fold higher than that from ^{90}Y. Microdosimetry calculations for real tumor systems and microdistribution can now be done with Monte Carlo calculations based on cell positions and isotope autoradiograph distribution using digitalized computer images (1). These types of microdosimetry calculations based on our model are in progress. Humm *et al.* (11) also calculated the relative effectiveness of these radioisotopes confined to a blood vessel surrounded by a cylinder (r = 100 μm) of tumor cells. The results show that at 1.8 MBq/g about 68% of the cells outside the vessel would not be hit by α particles emitted from ^{211}At. The value plateaued at about 40% unhit cells as the dose was increased. This result is due to the limited path length of the α-particle.

From a practical aspect, experiments with ^{213}Bi in the mouse lung system show that tumors ≥5,000 cells could not be cured (Table 4; 15). These tumors were estimated to have cells at least 10–12 cell diameters from the nearest blood vessel in lung and thus about 100 μm from the ^{213}Bi delivered by MAb 201B. Because the path length of the β particle from ^{90}Y is much longer, the tumor cell killing should not be limited to small tumors. The data (Table 4 and Fig. 1) show that although ^{90}Y is slightly more effective than ^{213}Bi for larger tumors (up to ~2,000 cells) the treatment still fails for larger tumors (~5,000 cells), even though these tumor cells receive an absorbed dose of over 50 Gy uniformly distributed throughout the lung (compare Table 2 and Table 4). It is possible that cells in large tumors are hypoxic and escape radiation-induced death or that the tumor burden is so large at the time of treatment that the residual fraction of nonlethally irradiated cells is too great a burden for the animals immune systems to clear (12). More sophisticated estimates of absorbed dose coupled with an understanding of tumor cell growth kinetics may explain these discrepancies.

Several examples of ^{90}Y MAb RIT have been published (7, 19, 27, 29). These experiments show that in leukemias the delivery of ^{90}Y to lymphoid cells can be effective in reducing tumor growth (28). Studies on solid tumor therapy in mice indicate that injected activities of 3.7–10 MBq per mouse are necessary to induce tumor regression. These doses were marginally tolerated in BALB/c mice in our system. Others have estimated 9–11 MBq ^{90}Y MAb as maximum tolerated doses (2, 7, 20). In BALB/c mice, doses of 2–4 MBq of ^{90}Y MAb 201 resulted in long-term damage in lungs due to fibrosis (at ~60 days), whereas higher doses (~10 MBq) resulted in lung hemorrhage and death at about 20 days postinjection. Damage to the animals' immune systems was also noted with ^{90}Y and could be due to cross-dose from the lung to bone marrow and other lymphoid sites. Yttrium-90 MAb 201B was found to be toxic in SCID mice. Injected activities of 2 MBq were lethal within 20 days postinjection. Because the animals are already severely immunodeficient, damage to the immune system is an unlikely cause of death. Damage to lung tissue resulting in hemorrhage is more likely. For this system of treatment of micrometasteses to be effective, a way to prevent collateral lung damage must be found. Our current working hypothesis is that lung fibrosis results from an inflammatory cascade starting with induction of TNFα production early after irradiation. Attempts to inhibit these effects are in progress.

The treatment system employed in this work utilizes a specific MAb that targets normal lung vasculature. Most of the tumors are in the lung because of the IV injection of the tumor cells. An optimal system would use a targeting agent specific for tumor vasculature. We predict that if such specific agents are found, vascular-targeted RIT, particularly for small tumors, will be effective and curative. The efficient delivery of radioisotope to the tumor area is the key. We are currently developing better vascular targeting molecules identified by the use of phage display libraries.

Specific vascular targeting results in destruction of the blood supply system as well as the tumor cells themselves. The α-emitter ^{213}Bi is the best choice for treatment of small tumors in the mouse, because it causes minimal collateral damage due to cross fire. The specific vascular targeting of β-emitters, such as ^{90}Y, may prove to be a better choice in humans in whom tumors and organs are larger, and spacing between specific targets and adjacent normal tissue may be greater.

We thank Trish Lankford, Linda Foote, and Arnold Beets for help with the animal studies and Jim Wesley for excellent histology work. Drs. Russ Knapp and Peggy Terzaghi-Howe added useful comments in review of the manuscript. This work was supported by an ORNL Laboratory Directors Research and Development award and by grants from DOE (ERKP 038) and NCI Office on Women's Health (IAA No. 97-053).

References

1. Akabani G. and Zalutsky M. R. (1997) Microdosimetry of astatine-211 using histological images: Application to bone marrow. *Radiat. Res.* **148,** 599–607.
2. Antoniw P., Farnsworth A. P. H., Turner A., Haines A. M. R., Mountain A., Mackintosh J., Shochat D., Humm J., Welt S., Old L. J., Yarranton G. T. and King D. J. (1996) Radioimmunotherapy of colorectal carcinoma xenografts in nude mice with yttrium-90 A33 IgG and Tri-Fab (TFM). *Brit. J. Cancer* **74,** 513–524.
3. Boll R. A., Mirzadeh S. and Kennel S. J. (1997) Optimization of radiolabeling of immunoproteins with ^{213}Bi. *Radiochim. Acta* **79,** 145–149.
4. Brechbiel M. W. and Gansow O. A. (1992) Synthesis of C-functionalized *trans*-cyclohexyldiethylene-triaminepentacetic acids for labeling of monoclonal antibodies with the bismuth-212 α-particle emitter. *J. Chem. Soc. Perkin Trans. 1.* **1,** 1173–1178.
5. Briesmeister J. (1993) *MCNP—A general Monte Carlo n-particle transport code. MCNP User's Manual.* Los Alamos National Laboratory, Los Alamos, TX.
6. Buchsbaum D. J., Langmuir V. K. and Wessels B. W. (1993) Experimental radioimmunotherpy. *Med. Phys.* **20,** 551–567.
7. Buchsbaum D. J., Lawrence T. S., Roberson P. L., Heidorn D. B., Ten Haken R. K. and Steplewski Z. (1993) Comparison of ^{131}I- and ^{90}Y-labeled monoclonal antibody 17-1A for treatment of human colon cancer xenografts. *Int. J. Radiat. Oncol. Biol. Phys.* **25,** 629–638.
8. Foster D. and Barrett P. (in press) Developing and testing integrated multicompartment models to describe a single-input multiple-output study using the SAAM II software system. *Proceedings of the Sixth International Radiopharmaceutical Dosimetry Symposium*, Oak Ridge Institute for Science and Educations, Oak Ridge, TN.
9. Giard D. J., Aaronson S. A., Todaro G. J., Arnstein P., Kersey J. H., Dosik H. and Parks W. P. (1973) *In vitro* cultivation of human tumors: Establishment of cell lines derived from a series of solid tumors. *J. Natl. Cancer Inst.* **51,** 1417–1423.
10. Hui T., Fisher D. R., Kuhn J. A., Williams L. E., Nourigat C., Badger C. C., Beatty B. G. and Beatty J. D. (1994) A mouse model for

calculating cross-organ beta doses from yttrium-90-labeled immunoconjugates. *Cancer* **73**(suppl.), 951–957.
11. Humm J. L. (1987) A microdosimetric model of astatine-211 labeled antibodies for radioimmunotherapy. *Int. J. Radiat. Oncol. Biol. Phys.* **13,** 1767–1773.
12. Kennel S. J., Boll R., Stabin M., Schuller H. M. and Mirzadeh S. (in press) Radioimmunotherapy of micrometastases in lung with targeted ^{213}Bi. *Brit. J. Cancer.*
13. Kennel S. J., Lankford T., Hughes B. and Hotchkiss J. A. (1988) Quantitation of a murine lung endothelial cell protein, P112, with a double monoclonal antibody assay. *Lab. Invest.* **59,** 692–701.
14. Kennel S. J. and Mirzadeh S. (1997) Vascular targeting for radioimmunotherapy with ^{213}Bi. *Radiochim. Acta* **79,** 87–91.
15. Kennel S. J. and Mirzadeh S. (1998) Vascular targeted radioimmunotherapy with ^{213}Bi—An α-particle emitter. *Nucl. Med. Biol.* **25,** 241–246.
16. Kozak R. W., Raubitschek A., Mirzadeh S., Brechbiel M. W., Junghaus R., Gansow O. A. and Waldmann T. A. (1989) Nature of the bifunctional chelating agent used for radioimmunotherapy with Yttrium-90 monoclonal antibodies: Critical factors in determining *in vivo* survival and organ toxicity. *Cancer Res.* **49,** 2639–2644.
17. Loevinger R., Budinger T. and Watson E. (1988) *MIRD Primer for Absorbed Dose Calculations*. Society for Nuclear Medicine, 128 pp.
18. Mordenti H. (1986) Man versus beast: Pharmacokinetic scaling in mammals. *J. Pharm. Sci.* **75,**1028–1040.
19. Morton B. A., Beatty B. G., Mison A. P., Wanek P. M. and Beatty J. D. (1990) Role of bone marrow transplantation in ^{90}Y antibody therapy of colon cancer xenografts in nude mice. *Cancer Res.* **50,** 1008s–1010s.
20. Muthuswamy M. S., Roberson P. L., Ten Haken R. K. and Buchsbaaum D. J. (1996) A quantitative study of radionuclide characteristics for radioimmunotherapy from 3D reconstructions using serial autoradiography. *Int. J. Radiat. Oncol. Biol. Phys.* **35,** 165–172.
21. Press O. W., Shan D., Howell-Clark J., Eary J., Appelbaum F. R., Matthews D., King D. J., Haines A. M. R., Hamann P., Hinman L., Shochat D. and Bernstein I. D. (1996) Comparative metabolism and retention of iodine-125, yttrium-90, and indium-111 radioimmunoconjugates by cancer cells. *Cancer Res.* **56,** 2123–2129.
22. Roeske J. C. and Stinchcomb T. G. (1997) Dosimetric framework for therapeutic alpha-particle emitters. *J. Nucl. Med.* **38,** 1923–1929.
23. Sharkey R. M., Motta-Hennessy C., Gansow O. A., Brechbiel M. W., Fand I., Griffiths G. L., Jones A. L. and Goldenberg D. M. (1990) Selection of a DTPA chelate conjugate for monoclonal antibody targeting to a human colonic tumor in nude mice. *Int. J. Cancer* **46,** 79–85.
24. Siegel J. A. and Stabin M. G. (1994) Absorbed fractions for electrons and beta particles in spheres of various sizes. *J. Nucl. Med.* **35,** 152–156.
25. Spector W. (1956) *Handbook of Biological Data.* W. B. Saunders, Baltimore.
26. Terzaghi-Howe M. (1987) Inhibition of carcinogen-altered rat tracheal epithelial cell proliferation by normal epithelial cell proliferation by normal cells *in vivo*. *Carcinogenesis* **8,** 145–150.
27. Vergote I., Larsen R. H., de Vos L., Nesland J. M., Bruland O., Bjorgum J., Alstad J., Tropé C. and Nustad K. (1992) Therapeutic efficacy of the alpha-emitter ^{211}At bound on microspheres compared with ^{90}Y and ^{32}P colloids in a murine intraperitoneal tumor model. *Gynecol. Oncol.* **47,** 366–372.
28. Waldmann T. A., White J. D., Carrasquillo J. A., Reynolds J. C., Paik C. H., Gansow O. A., Brechbiel M. W., Jaffe E. S., Fleisher T. A., Goldman C. K. *et al.* (1995) Radioimmunotherapy of interleukin-2R alpha-expressing adult T-cell leukemia with Yttrium-90-labeled anti-Tac. *Blood* **86,** 4063–4075.
29. Wong J. Y. C., Williams L. E., Demidecki A. J., Wessels B. W. and Yan X. W. (1991) Radiobiologic studies comparing Yttrium-90 irradiation and external beam irradiation *in vitro*. *Int. J. Radiat. Oncol. Biol. Phys.* **20,** 715–722.
30. Wu C., Kobayashi H., Sun B., Yoo T. M., Paik C. H., Gansow O. A., Carrasquillo J. A., Pastan I., and Brechbiel M. W. (1997) Stereochemical influence on the stability of radio-metal complexes *in vivo*. Synthesis evaluation of the four steroisomers of 2-(*p*- Nitrobenzyl)-*trans*-CyDTPA. *Bioorganic Med. Chem.* **5**(10), 1925–1934.
31. Yoriyaz H. and Stabin M. (1997) Electron and photon transport in a model of a 30-g mouse. *J. Nucl. Med.* **38**(suppl.), 228.
32. Zalutsky M. R. and Bigner D. (1996) Radioimmunotherapy with α-particle emitting radioimmuno-conjugates. *Acta Oncol.* **35,** 373–379.